

Electronic supporting information

Selective sensing of dihydrogen phosphate anion by a fluorescent tetranuclear pentacoordinated zinc(II) complex

Zhanfen Chen, Xiaoyong Wang, Jingwen Chen, Xiaoliang Yang, Yizhi Li,
and Zijian Guo

Table of Contents:

- Fig. S1 ESMS spectrum (above), the isotopic distribution pattern (middle) and the simulated distribution pattern (bottom) of the peaks for complex **I** (methanol, positive mode).
- Fig. S2 ^1H NMR spectrum of complex **I** (CD_3CN). The labeled peaks correspond to the minor tautomers of the complex. The ethanol and ether peaks are due to the impurity of the deuterated solvent.
- Fig. S3 ^1H NMR spectra (upfield part) of complex **I** ($\text{CD}_3\text{OD:D}_2\text{O} = 5:2$, 25°C) alone (A) and with H_2PO_4^- (B) in a 1:2 molar ratio. The labeled peaks correspond to the minor tautomers of the complex.
- Fig. S4 UV-Vis spectrum of complex **I** ($45 \mu\text{M}$, methanol).
- Fig. S5 Fluorescence spectrum of complex **I** ($45 \mu\text{M}$, methanol, $\lambda_{\text{ex}} = 298 \text{ nm}$).
- Fig. S6 Fluorescence emission changes of **L** ($\lambda_{\text{ex}} = 298 \text{ nm}$, $45 \mu\text{M}$, methanol) upon addition of H_2PO_4^- ($0\text{--}135 \mu\text{M}$, sodium salt) at room temperature.
- Fig. S7 UV-Vis absorption spectra of **L** ($45 \mu\text{M}$, methanol) upon addition of H_2PO_4^- ($0\text{--}135 \mu\text{M}$, sodium salt) at room temperature.
- Fig. S8 UV (A) and fluorescence (B) spectra changes of the tetranuclear complex $[\text{Zn}_4^{II}(\text{L}-3\text{H})_2](\text{ClO}_4)_2 \cdot 3.5\text{H}_2\text{O}$ ($45 \mu\text{M}$, methanol) upon addition of HCl at room temperature. The final concentrations of HCl are 0, 24, 48, 72, 96, 120, 144, 168, and $192 \mu\text{M}$, respectively.
- Fig. S9 ESMS (above, methanol) and ^1H NMR spectra (bottom, CDCl_3) of **L**.
- Table S1 Selected bond distances (\AA) and bond angles ($^\circ$) for $[\text{Zn}_4^{II}(\text{L}-3\text{H})_2](\text{ClO}_4)_2 \cdot 3.5\text{H}_2\text{O}$.

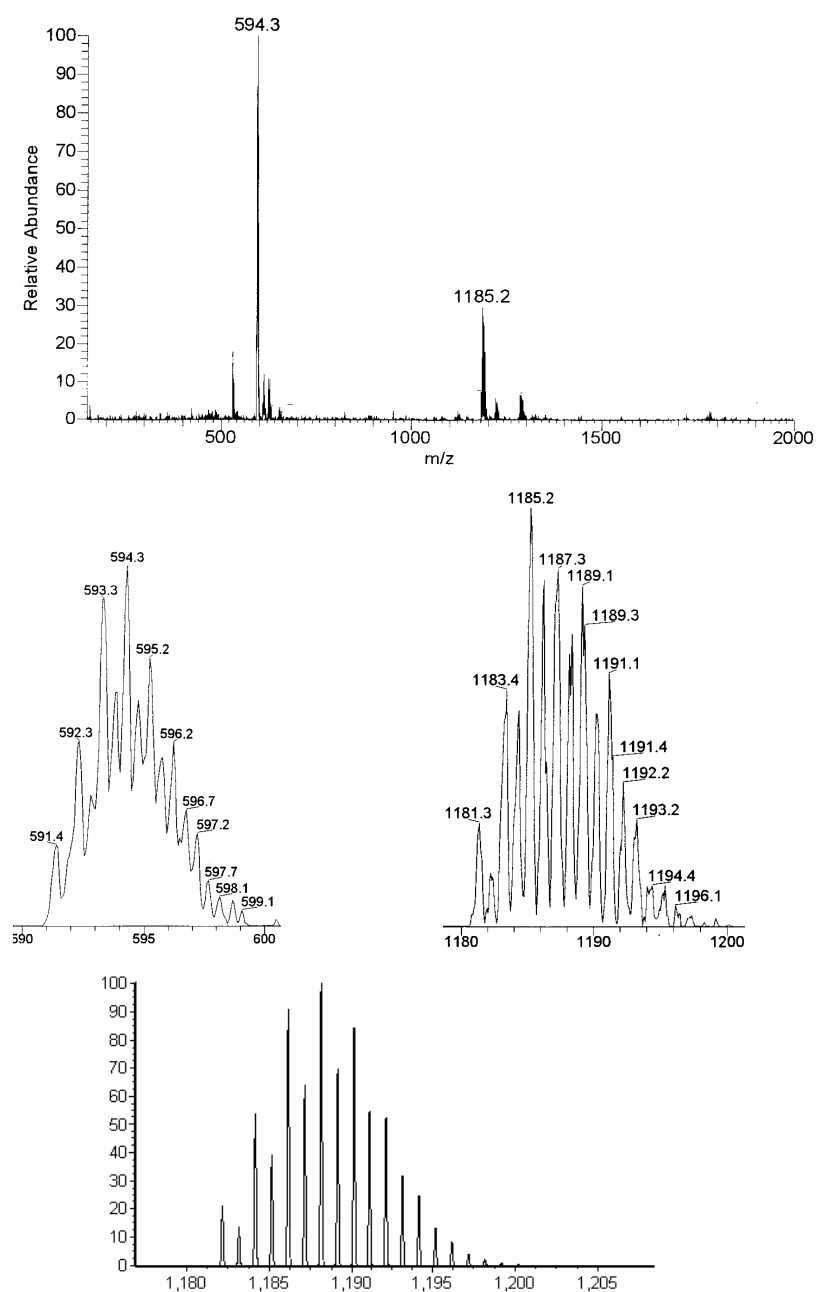


Fig. S1 ESMS spectrum (above), the isotopic distribution pattern (middle) and the simulated distribution pattern (bottom) of the peaks for complex **I** (methanol, positive mode).

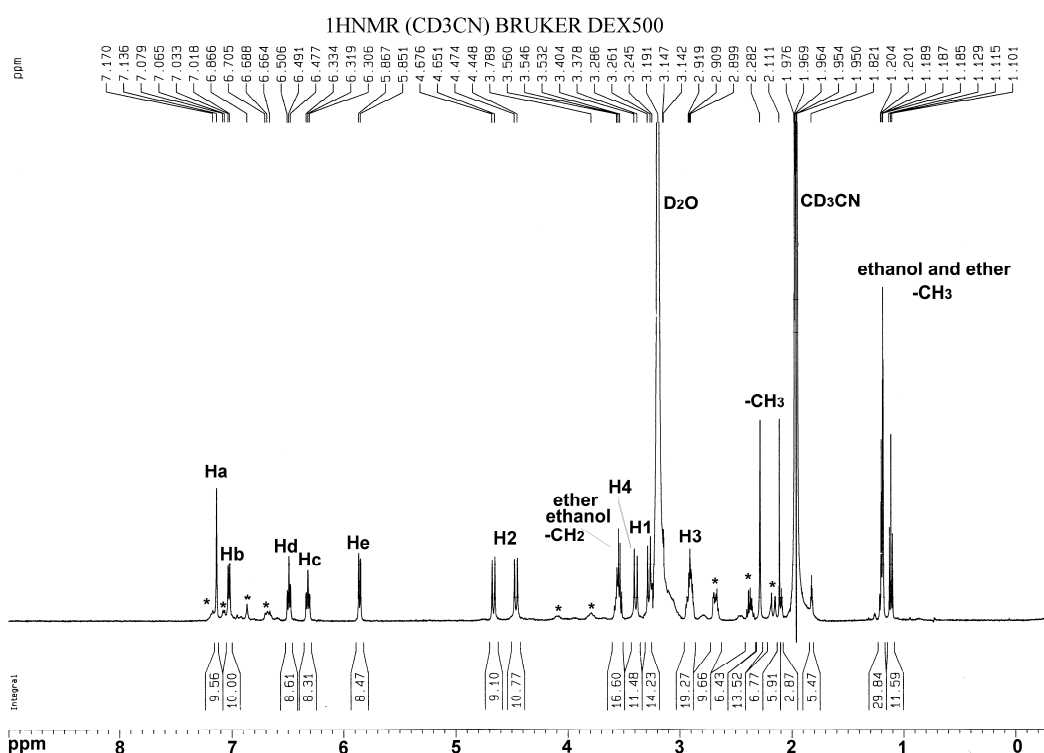


Fig. S2 ^1H NMR spectrum of complex **I** (CD_3CN). The labeled peaks correspond to the minor tautomers of the complex. The ethanol and ether peaks are due to the impurity of the deuterated solvent.

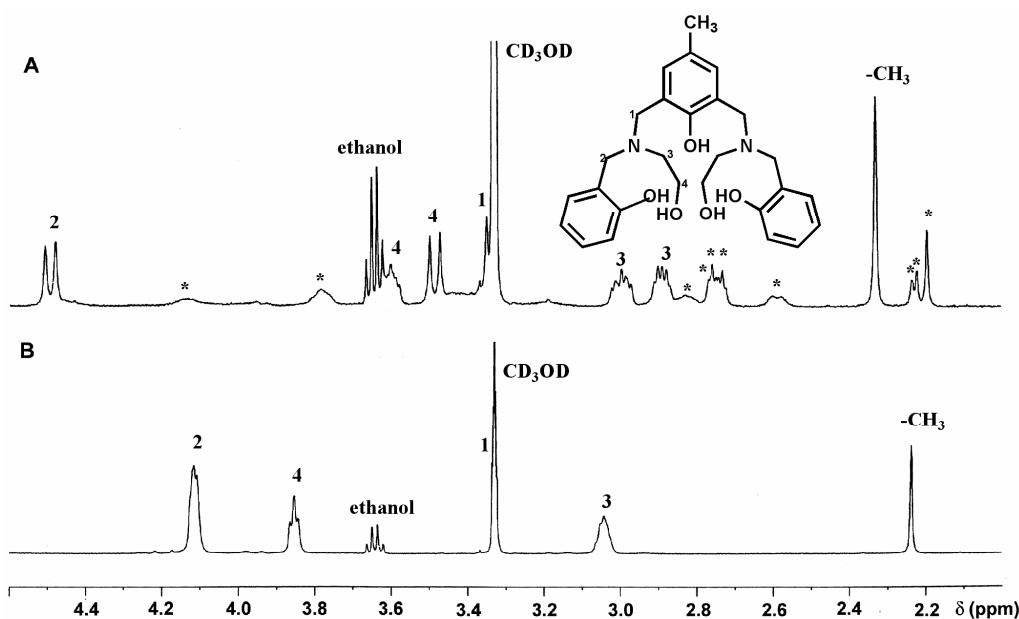


Fig. S3 ^1H NMR spectra (upfield part) of complex **I** ($\text{CD}_3\text{OD}:\text{D}_2\text{O} = 5:2$, 25°C) alone (A) and with H_2PO_4^- (B) in a 1:2 molar ratio. The labeled peaks correspond to the minor tautomers of the complex.

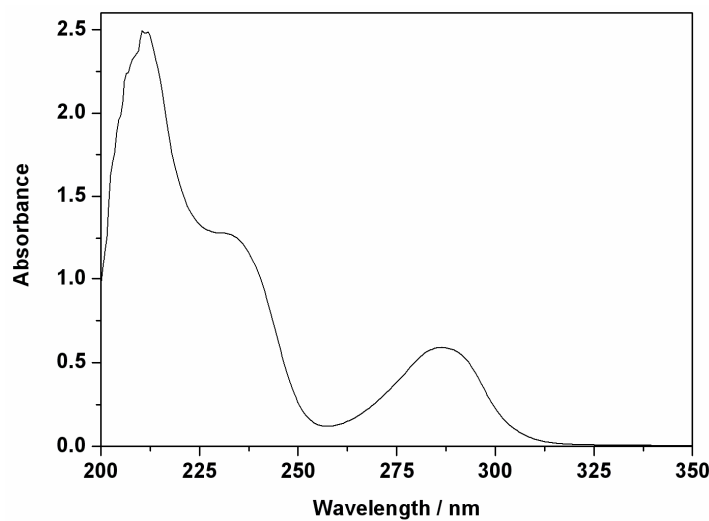


Fig. S4 UV-Vis spectrum of complex **I** (45 μ M, methanol).

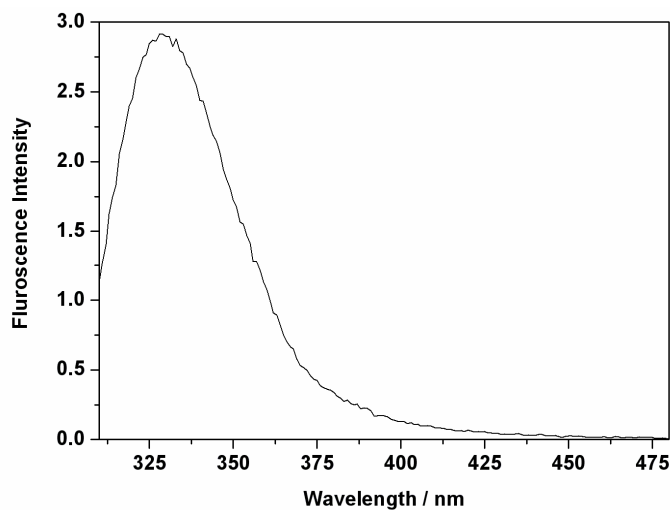


Fig. S5 Fluorescence spectrum of complex **I** (45 μ M, methanol, $\lambda_{\text{ex}} = 298$ nm).

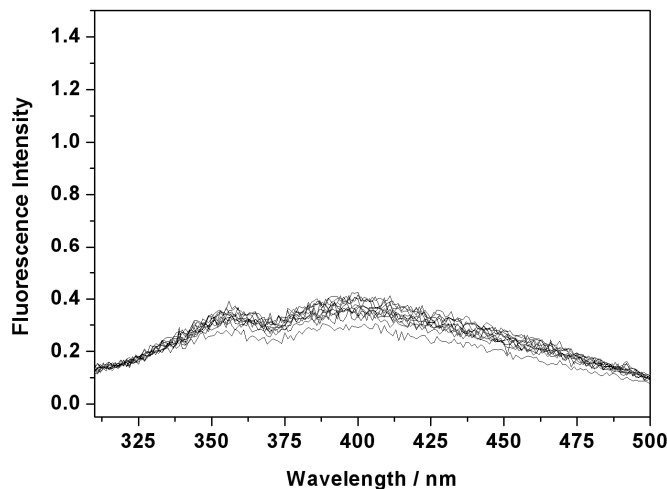


Fig. S6 Fluorescence emission changes of **L** ($\lambda_{\text{ex}} = 298$ nm, 45 μ M, methanol) upon addition of

H_2PO_4^- (0–135 μM , sodium salt) at room temperature.

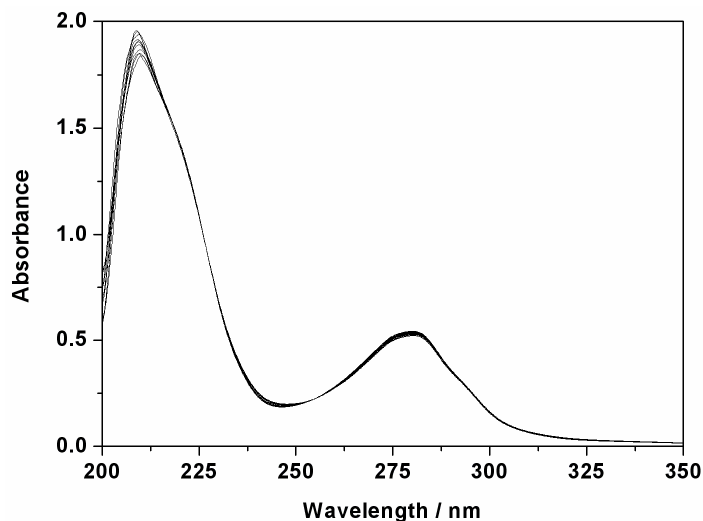


Fig. S7 UV-Vis absorption spectra of **L** (45 μM , methanol) upon addition of H_2PO_4^- (0–135 μM , sodium salt) at room temperature.

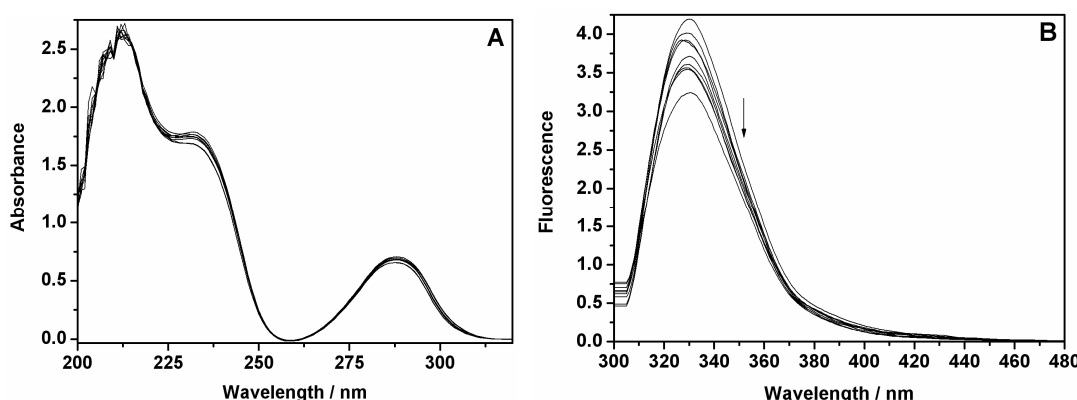


Fig. S8 UV (A) and fluorescence (B) spectra changes of the tetrานuclear complex $[\text{Zn}_4^{\text{II}}(\text{L}-3\text{H})_2](\text{ClO}_4)_2 \cdot 3.5\text{H}_2\text{O}$ (45 μM , methanol) upon addition of HCl at room temperature. The final concentrations of HCl are 0, 24, 48, 72, 96, 120, 144, 168, and 192 μM , respectively.

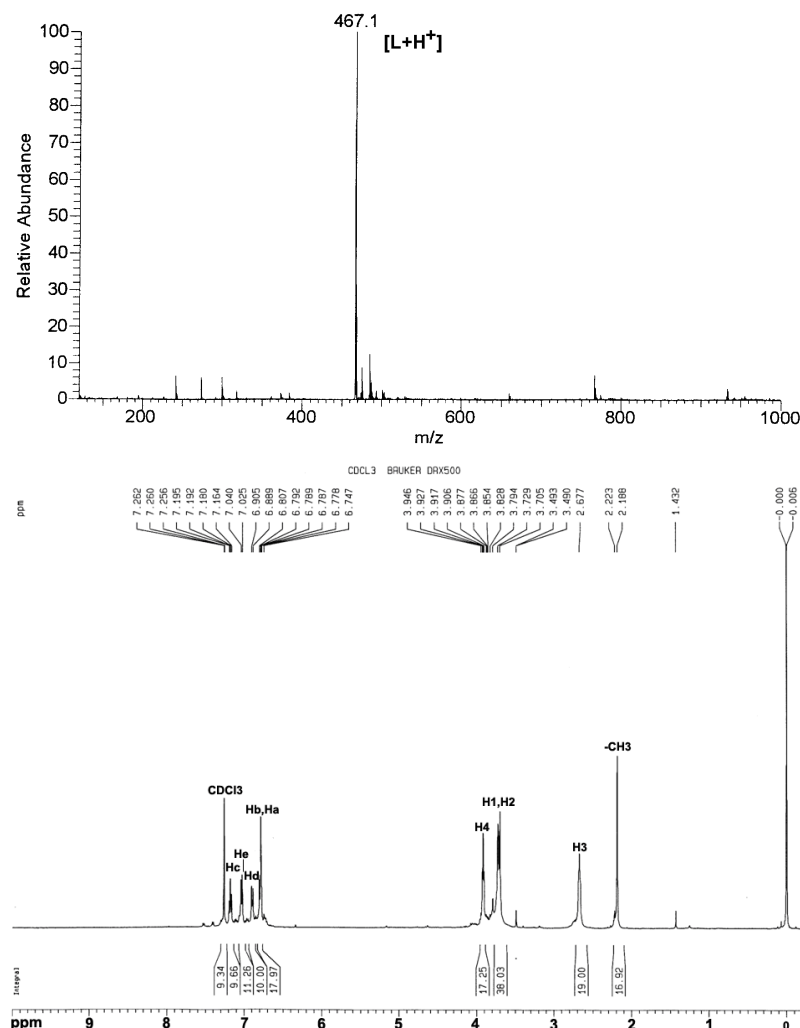


Fig. S9 ESMS (above, methanol) and ¹H NMR spectra (bottom, CDCl₃) of L.

Table S1 Selected bond distances (\AA) and bond angles ($^\circ$) for $[\text{Zn}_4^{\text{II}}(\text{L}-3\text{H})_2](\text{ClO}_4)_2 \cdot 3.5\text{H}_2\text{O}$.

Bond Lengths			
Zn(1)–O(2)	1.971(3)	Zn(2)–O(2)	2.024(3)
Zn(1)–O(4)	1.971(3)	Zn(2)–O(7)	2.122(3)
Zn(1)–O(5)	2.023(3)	Zn(2)–O(8)	2.008(3)
Zn(1)–O(6)	2.123(3)	Zn(2)–O(9)	2.023(3)
Zn(1)–N(4)	2.130(3)	Zn(2)–N(3)	2.141(4)
Zn(3)–O(1)	1.966(3)	Zn(4)–O(1)	2.013(3)
Zn(3)–O(8)	2.020(3)	Zn(4)–O(3)	2.172(3)
Zn(3)–O(9)	1.990(3)	Zn(4)–O(4)	2.022(3)
Zn(3)–O(10)	2.120(3)	Zn(4)–O(5)	1.961(3)
Zn(3)–N(2)	2.148(3)	Zn(4)–N(1)	2.092(3)
Zn(1)…Zn(2)	3.637(1)	Zn(1)…Zn(4)	3.084(1)
Zn(2)…Zn(3)	3.096(1)	Zn(3)…Zn(4)	3.626(1)
Bond Angles			
O(2)–Zn(1)–O(4)	114.14(11)	O(2)–Zn(2)–O(7)	113.33(11)
O(2)–Zn(1)–O(5)	110.37(11)	O(2)–Zn(2)–O(8)	112.66(11)
O(2)–Zn(1)–O(6)	103.46(12)	O(2)–Zn(2)–O(9)	106.56(11)
O(2)–Zn(1)–O(4)	95.76(12)	O(2)–Zn(2)–N(3)	95.90(10)
O(4)–Zn(1)–O(5)	78.14(10)	O(7)–Zn(2)–O(8)	133.83(11)
O(4)–Zn(1)–O(6)	91.34(11)	O(7)–Zn(2)–O(9)	91.82(10)
O(4)–Zn(1)–N(4)	150.10(12)	O(7)–Zn(2)–N(3)	78.82(11)
O(5)–Zn(1)–O(6)	146.00(12)	O(8)–Zn(2)–O(9)	78.97(11)
O(5)–Zn(1)–N(4)	92.10(12)	O(8)–Zn(2)–N(3)	92.76(11)
O(6)–Zn(1)–N(4)	81.06(12)	O(9)–Zn(2)–N(3)	157.54(11)
O(1)–Zn(3)–O(8)	112.66(11)	O(1)–Zn(4)–O(3)	102.25(10)
O(1)–Zn(3)–O(9)	107.87(11)	O(1)–Zn(4)–O(4)	110.15(11)
O(1)–Zn(3)–O(10)	104.82(12)	O(1)–Zn(4)–O(5)	113.42(11)
O(1)–Zn(3)–N(2)	93.67(12)	O(1)–Zn(4)–N(1)	96.77(11)
O(8)–Zn(3)–O(9)	79.46(11)	O(3)–Zn(4)–O(4)	147.53(11)
O(8)–Zn(3)–O(10)	92.47(11)	O(3)–Zn(4)–O(5)	91.00(10)
O(8)–Zn(3)–N(2)	153.66(12)	O(3)–Zn(4)–N(1)	80.65(12)
O(9)–Zn(3)–O(10)	146.96(12)	O(4)–Zn(4)–O(5)	78.41(11)
O(9)–Zn(3)–N(2)	92.11(12)	O(4)–Zn(4)–N(1)	93.16(12)
O(10)–Zn(3)–N(2)	81.02(12)	O(5)–Zn(4)–N(1)	149.77(11)
Zn(3)–O(1)–Zn(4)	131.39(14)	Zn(1)–O(2)–Zn(2)	131.08(14)
Zn(1)–O(4)–Zn(4)	101.13(12)	Zn(1)–O(5)–Zn(4)	101.45(11)
Zn(2)–O(8)–Zn(3)	100.44(12)	Zn(2)–O(9)–Zn(3)	101.96(12)